TECHNICAL ARTICLE

Analysis of Breathing Cracks Using Vibrations

G.E. Carr, L.F. Jaureguizahar, and M.D. Chapetti

Laboratory of Experimental Mechanics, INTEMA (Research Institute for Materials Science and Technology), CONICET - Mar del Plata National University, Mar del Plata BF7608FDQ, Argentina

Keywords
Fatigue, Dynamic Testing, Strain Gages

Correspondence
G.E. Carr,
Laboratory of Experimental Mechanics,
INTEMA (Research Institute for Materials Science and Technology),
CONICET - Mar del Plata National University,
Av. Juan B. Justo 4302,
Mar del Plata BF7608FDQ, Argentina
Email: gecarr@fi.mdp.edu.ar

Received: September 9, 2010; accepted: January 10, 2012

doi:10.1111/j.1747-1567.2012.00816.x

Abstract

The influence of half-ellipse-shaped fatigue cracks and machined through-thickness cuts on the impact response of cantilever beam samples were analysed using the Finite Element Method and compared to experimental data for different crack depths. The effect of sample width was analysed for geometries with fatigue cracks (aspect ratio $a/c = 0.45$) and through-thickness cuts (rectangular cracks). The differences between both types of damage were analysed numerically and experimentally. The effect of sample width was studied and it was found that the behaviour of the cantilever with a fatigue-crack approaches that of the saw cut sample when the fatigue crack reaches the edges of the test piece. Acceleration data were analysed using the Fast Fourier Transform algorithm and Power Density Spectra (PSD) were obtained. For fatigue-cracked samples, harmonics of the frequencies of natural modes of oscillation were found. Analytical modelling was done using a mass-spring-damper system for studying the bilinear behaviour of the stiffness element. Harmonics found were assigned to the breathing behaviour of the crack. The detection threshold using frequency shifts inspection was twice as high as using spectral analysis. This would allow crack detection at half of the fatigue life of the specimen.

Introduction

The vibration of structures and components has been extensively used to detect defects and cracks because they affect both the way they vibrate and their natural frequencies. These methods to measure damage can be put together in three groups: (1) modal testing: techniques that study the natural modes shape changes due to damage; (2) vibration-based: methods that use the time-based signal or modelling; (3) non-traditional: methods such as fuzzy logic, neural networks, etc.

Modal vibration analysis was based on the fact that cracks alter the stress distributions for each mode shape in a different way.[1] When cracks develop on rotating shafts, mode coupling occurs. This fact was used successfully to detect cracks in rotating shafts using a combination of vibration and fracture mechanics.[2] This field of study gave quite an amount of work.[3–6] Other authors used earlier stress fields because of cracks[7] with an energy approach in combination with fracture mechanics for analysing the behaviour of cracked beams. Inverse methods were also used to analyse the vibrational response of cracked prismatic beams[8–12] by calculating the modal shapes of vibration and the eigen frequencies of Timoshenko beams of Euler–Bernoulli beams and comparing these results to experimental data.

Open real cracks surfaces are separated in surface tensile stress and closed in compressive stress. This leads to a nonlinear bending stiffness of the beam. Half-elliptical-shaped cracks, the most common geometry for this defect, are characterised by their aspect ratio a/c, "a" being their depth and "c" half their length measured on the surface. A crack with an aspect ratio equal to null means a through-thickness crack. When authors use a theoretical two-dimensional beam model, they are forced to make through-thickness cuts on their experimental samples to be closer to the analytical results. Silva and Gómez[13] found that the same change in natural frequency due to a through-thickness cut could be found with a semi-elliptical crack of half its depth. The behaviour of a breathing crack leads to a bilinear response in the beam bending stiffness. Other authors studied the spectral signature of bilinear oscillators,[14] which behave in a similar way as beams with a breathing crack.[15] This behaviour represents a hard issue in the Finite Element Method modelling (FEM) of the beam response.[4]

Authors often modelled the cracks as through-thickness cuts but the influence of the geometry of the discontinuity on the modelling results was seldom reported.

Most of the experimental work found in literature used samples with cracks of depth-to-thickness ratio, a/h, equal to or greater than 0.1, ''h'' being the sample thickness. Cracks that have low depth ratios are difficult to detect when using the first modes natural frequencies shift or modal analysis. Nevertheless, the responses of the nonlinear behaviour of beams with such small cracks are more distinguishable than the change on natural frequencies.[12] Owolabi et al.[16] have found a decrease as small as 1% in the first mode vibration frequency for cracks of depth ratio $a/h = 0.1$. Different methods, such as the analysis of the slope of antiresonance curves[17] or frequency response functions[18] were used with cracks of depth ratios equal and greater than 0.1, lacking in sensibility when depth ratio was smaller.

In this work, the difference between fatigue cracks and through-thickness cuts on the free vibrating response of cantilever beams was studied using the FEM and free vibration impact responses. The relation between fatigue cracks and sample width and the influence of the geometry of the through-thickness cuts on modelling results were studied.

In addition, the spectral analysis technique was used and compared to natural frequencies shift inspection technique.

Experimental and Numerical Analysis Procedure

Materials, methods, and experimental tests

The influences of naturally initiated surface cracks and through-thickness cuts on vibrational responses were studied by using tee-shaped samples cut from two tee-welded plates. The tee-shaped samples of 25.4-mm thick base plate and 12.7-mm thick cantilever plate were made by MIG welding using 310 A current and 30 V voltage. The plates material was A36 steel and the welding speed was 0.4 m·min^{-1}. Samples width was $B = 47$ mm.

The samples for fatigue-cracks study were fixed by the base plate and submitted to bending stress cycling with $R = \sigma_{MIN}/\sigma_{MAX} = 0.2$ stress amplitude ratio at 10 Hz, using a walking beam type fatigue testing machine, as shown in Fig. 1, for fatigue cracks to grow at the stress concentrators at the weld toe. Previous exploratory tests were carried out to determine the range of stresses needed for the propagation of fatigue cracks under elastic regime. It was found that cracks developed for stress amplitudes higher than 240 MPa and run-outs were obtained for lower ranges. Hence, the oscillating forces applied to the cantilever were chosen so as to develop 250 MPa of stress amplitude at the weld toe with a maximum stress below the material yield stress (280 MPa) to ensure elastic propagation of cracks and to avoid plastic propagation regime. The experimental set-up for this type of test sample is shown in Fig. 2.

For every 0.5-mm of crack growth, the alternating stress was released in order to perform free vibration impact tests. The stress at the weld toe was measured by strain gages and the crack depth was measured on-line by means of the same strain gages using an indirect method detailed in *Crack Depth and Shape Measuring* section.

The experimental set-up of samples for studying the through-thickness cuts influence on vibration response is shown in Fig. 3. These samples were cut using a 3-mm thick rotary saw to ensure a uniform cut depth and width.

For vibration response testing, three driving points were chosen so as to excite different eigen modes. These driving points are located at the end of the cantilever part of the samples, defined as corner, centre and corner, as shown in Figs. 2(d) and 3(d). Driving points 1 and 3 excite both bending and

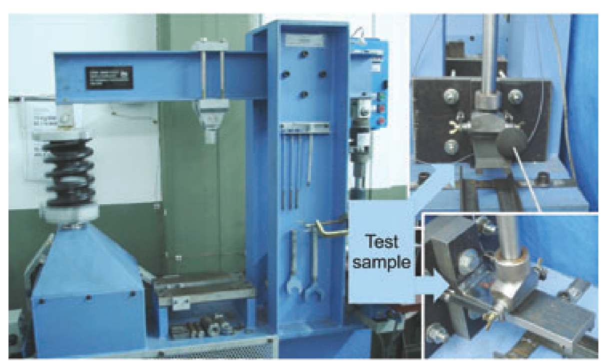

Figure 1 Fatigue testing machine of the walking beam type used for the generation of fatigue cracks on cantilever beam specimens. Fatigue cracks were grown by alternating tensile stresses on the top surface of the specimens.

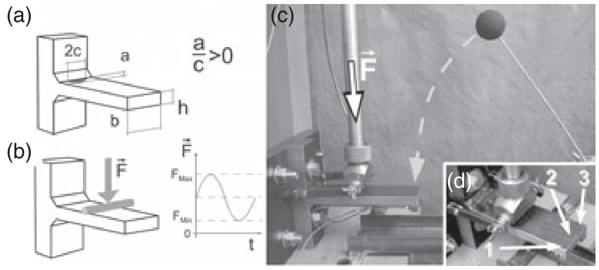

Figure 2 Experimental set-up for free vibration testing on samples with cracks of aspect ratio $a/c = 0.45$. (a) Schema showing the geometry of fatigue cracks. (b) Direction of the alternating force and force actuator for the generation of fatigue cracks. (c) Cantilever specimen positioned for the application of bending stresses for the growing fatigue cracks. Direction of the alternating force F, actuator, rubber ball for impact testing and accelerometers are shown. (d) The location of the driving points and the accelerometers fixed below cantilever end are shown.

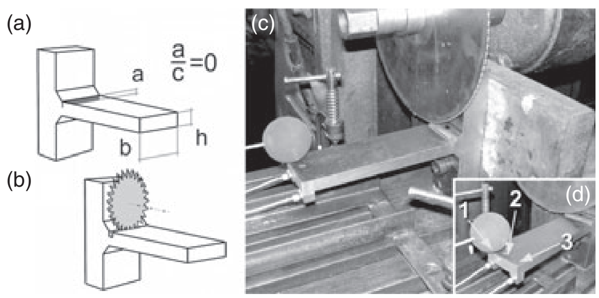

Figure 3 Experimental set-up for the creation of defects on samples of aspect ratio $a/c = 0$. (a) Schema showing the geometry of through-thickness cuts. (b) Schema showing the machining of through-thickness cuts. (c) Sample set-up showing the impact ball. (d) Detail of the driving points for impact testing. Location of accelerometers below the cantilever end.

twisting modes, while driving point number 2 excites mainly the bending modes. The crack detection and depth measuring technique was a set of strain gages attached to the surface of the cantilever where the highest stresses develop, close to the weld toe as shown in Fig. 4(a).

Crack depth and shape measuring

The depth and shape of the crack initiated by fatigue at the weld toe of the tee-shaped specimens were measured and monitored by an indirect multiple strain gage technique.

The strain gage crack depth measuring method was developed by Otegui et al.[19] firstly for two-dimensional analysis of fatigue cracks (Fig. 4(b)) but lately extended to three-dimensional analysis[20] with the aid of the FEM and the use of multiple strain gages (Fig. 4(c)). A later development by Jaureguizahar[21] lowered the threshold of detection of cracks down to 90 μm. This method relies on the fact that the tensile stress lines developed on a sample in bending stress are parallel to the surface of an intact sample but they are bent inwards by the growing of a crack from the sample surface. The detection of this effect can be monitored by a strain gage attached to the surface at a distance H from the crack mouth as it grows. When the sample is submitted to constant amplitude fatigue stress, the crack grows and the stress amplitude measured by the strain gage decreases, for what it can be compared to the intact sample stress amplitude.

Crack depth can be measured by using an initial calibration curve, shown in Fig. 4(d), obtained by previous experimental measurements, plotted as the normalized load slope, P/P_0, versus crack depth normalized to the distance to the crack mouth, a/H. The normalized load slope is the ratio of the actual loading cycle slope, $P = \Delta F/\Delta\varepsilon$, to the intact sample loading cycle slope, $P_0 = \Delta F_0/\Delta\varepsilon_0$, F being the load and ε the strain in $\mu\varepsilon$. The crack depth can be calculated in an indirect manner, using the fitting curve with the actual distance H between strain gage centre and crack mouth. Ink marks are made for each 1-mm interval of crack growth. After the sample failure the curve is re-calibrated to correct the starting point distances to each strain gage and each crack depth, a_i, using the ink marks. The minimum size of crack for detection is inversely proportional to the distance H_1 between the crack mouth and the strain gage. The upper limit for accurately measuring crack depth is proportional to H_1. For measuring a deeper crack with confidence, a strain gage at distance H_2 should be placed, but the threshold of detection for this strain gage is higher than the one for the strain gage at distance H_1. In order to measure the shape of the crack, a group of strain gages should be attached parallel to the expected crack opening since each strain gage measurement is affected by the stress field below it.

The advantage of this method is based on the possibility of measuring the crack depth while it is growing, allowing the researcher to stop every prescribed interval to perform vibration response measurements. The crack growth step for impact response testing was 0.5 mm.

This technique was chosen by the authors to measure the crack depth and shape throughout its growth and relating these data to the free vibration response.

Vibration data acquisition procedure

The influence of cracks on impact response study was carried out using software written in QtOctave environment.[22,23] Series of more than eight impacts

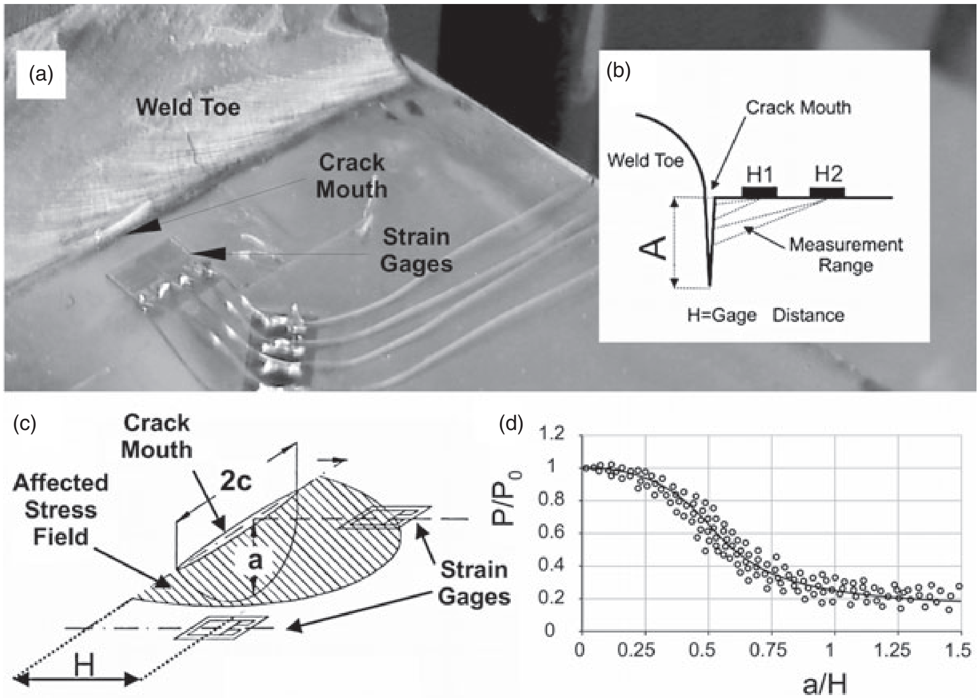

Figure 4 Schema showing the Indirect Method for crack depth measurement.[21] (a) Detail of the position of strain gages on the top of specimens surface. (b) Schema showing the crack depth measurement range for strain gages at different distances from the weld toe. (c) Stress field affected by the existence of a crack. (d) Calibration curve.

were done on the three driving points for each crack depth interval. The data collected were averaged for each driving point and crack depth step. The digital domain Fast Fourier Transform was applied to the data recorded.

The cantilever test samples were hit perpendicularly to the surface using a rubber ball weighing 66 ± 0.5 g, released from 210 ± 1 mm constant height to get a good signal-to-noise ratio. Samples were hit at the three driving points at impact velocities of 1.85 ± 0.2 m·s^{-1}. Each impact test was repeated at least nine times for each driving point for data averaging.

The equipment used for data acquisition was a National Instruments NI-SCXI-1530 and two Brüel and Kjaer, DeltaTron accelerometers, type 4507-001. Sampling frequency was chosen at 48 KHz with an analogue filter of 12 dB·octave^{-1} slope with cut-off set at 2.5 KHz. The accelerometers were fixed to the cantilever under driving points 1 and 3. The data gathered from each impact sequence were processed using the Fast Fourier Transform algorithm. The sampling frequency was 48 KHz and the data vector sizes were always long enough so as to ensure a frequency resolution[24] of at least ±0.37 Hz. Power spectral density graphs were obtained and averaged for the same crack depth and driving point.

Numerical modelling

Three-dimensional analysis was carried out for studying the influences of both semi-elliptical cracks (aspect ratio $a/c = 0.45$) and through-thickness slots ($a/c = 0$) on the samples eigen frequencies. The FEM software Abaqus(R) was used for numerical modelling.

A convergence study was performed previously to choose the appropriate size of elements. The elements size at the crack was 0.25 mm and not larger than 4 mm anywhere else in the models. The element types used were C3D4 (tetrahedral) because of their good adaptivity to the sample geometry and the gradient size of elements across the model. The values chosen for materials constants were: Young's Modulus, $E = 209$ GPa; Poisson's Modulus, $\nu = 0.3$; density, $\rho = 7800\ \mathrm{Kg \cdot m^{-3}}$. For the analysis of semi-elliptical cracks, the starting position for the cracks was chosen just at the weld toe, given that at that point the highest tensile stress amplitudes developed when the cantilever was submitted to fatigue in bending.

Four crack depths were chosen for FEM analyses in each condition: $a_1 = 1.5$ mm, $a_2 = 3$ mm, $a_3 = 4.25$ mm, and $a_4 = 5.5$ mm.

The main sample geometry used for modelling was the same as for laboratory testing. However, additional modelling was done using different shapes and widths of through-thickness cuts, as shown in Fig. 5(a–d). For through-thickness cut sample models geometries, width was kept constant: $B = 47$ mm. On the other hand, different sample models widths were used for fatigue cracked while keeping the crack aspect ratio constant (Fig. 5(e and f)). Values for width were: $B_1 = 20$ mm, $B_2 = 30$ mm, $B_3 = 47$ mm, and $B_4 = 75$ mm.

Results and Discussions

The FEM modelling results for samples with fatigue cracks of aspect ratio $a/c = 0.45$ are shown in Fig. 6. Modelling results for geometries with through-thickness cuts are shown in Fig. 7. In both figures, the natural frequencies of the first mode of vibration (vertical bending) are displayed for growing crack depth ratios.

From the experimental data collected, the frequencies of the first mode of vibration for through-thickness cut samples and fatigue-cracked samples are shown in both Figs. 6 and 7 for comparison between them and for modelling results.

From observing experimental data shown in both Figs. 6 and 7, it can be seen that the decrements of the samples natural frequencies provoked by fatigue cracks were smaller than those decrements generated by through-thickness cuts. This can be explained by the fact that the sample cross-sectional area affected by the through-thickness cut is greater than the area affected by a fatigue crack of the same depth as the former. The remaining cross-section had a different bending stiffness in each case.

It can be observed on modelling results shown in Fig. 6 that relative frequency shift versus relative crack depth curves were closer to the through-thickness cut samples curve for lower values of sample width. This can be explained by the fact that the fatigue cracks provoked by fatigue in bending are half-ellipse shaped throughout their growth until they reach the sample lateral surface, as shown schematically in Fig. 5(e). From this point onwards the crack would have a shape similar to the one shown in Fig. 5(f). This fatigue crack would act more like a through-thickness cut than like an elliptical-shaped crack.

In Fig. 7, it can be observed that through-thickness cut geometries modelling results were closer to

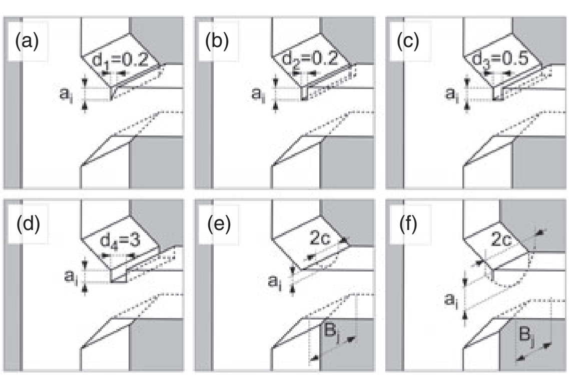

Figure 5 Schema showing the shape of through-thickness cuts ($a/c = 0$) and fatigue cracks ($a/c = 0.45$) on two different specimen widths used for three-dimensional modelling to study the influence of width and crack shape on the natural frequencies of the specimens.

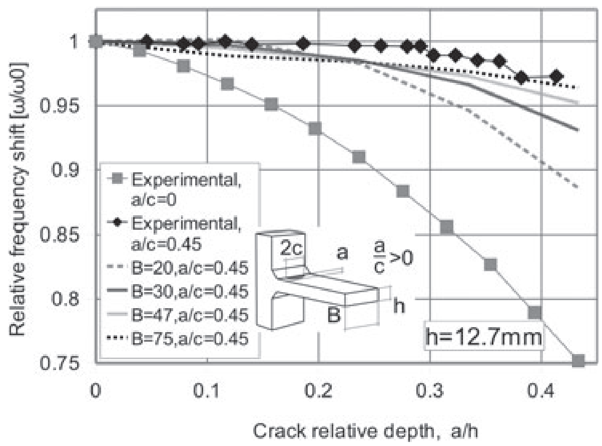

Figure 6 Experimental and three-dimensional modelling results for mode 1 frequency ratio versus different crack depths are shown. The influence of crack growth on the first natural frequency ratio for crack aspect ratios of $a/c = 0.45$ and different specimen widths B are shown.

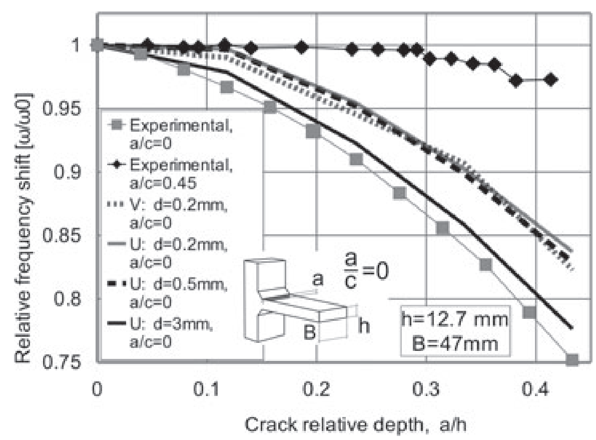

Figure 7 Experimental and three-dimensional modelling results for mode 1 frequency ratio and different crack depths are shown. The influence of through-thickness cuts (equivalent to hypothetical cracks with aspect ratio $a/c = 0$) for different cut shapes (U or V) and different depths, d, on first natural frequencies are shown.

experimental data when the geometry used for modelling contained a cut whose dimensions were equal to those of the actual cut done on the test samples. This fact shows that the experimental techniques for making test samples must be considered when modelling. In finite element results shown in Fig. 7, it can be seen that all frequency shifts due to through-thickness cracks were lower than those found experimentally. This can be due to the lack of rotary inertia of the elements used in modelling that would provoke an effect of artificially increasing the cantilever bending stiffness.

The experimental detection threshold for fatigue cracks using the natural frequency decrease was found at about 3.75 mm or 30% of the sample thickness. This value was considered not sufficient by the authors. In searching for a lower threshold, the Power Spectral Density (PSD) of the acceleration data was calculated for all the impact events. These results are shown in Fig. 8. In this figure, the energy corresponding to each frequency band is plotted against the axis of frequency and the frequencies of the principal modes of vibrating appear as peaks. These data were averaged for each crack growth step after measuring sequences of impacts onto the driving point 1. It can be observed that the crack growth affected mostly the bending modes, by decreasing their corresponding frequency peaks. Side bands were detected due to mode coupling. Taking $f1$ as the fundamental frequency for mode 1, there were peaks at frequencies $2{\cdot}f1$ and $3{\cdot}f1$ for crack depth greater than 1 mm, which were not predicted by FEM modelling. This effect can be due to the bilinear behaviour of the cantilever, after Zhang and Billings[15] and Bayly.[14] Also, Bovsunovsky and Matveev[12] proposed this theoretically. Additional numerical modelling was carried out to confirm this hypothesis. The exact solution for a 1-d.f. mass-spring-damper system was solved for a bilinear behaviour spring element. The differential equation governing the system motion was as follows:

$$\mathrm{d}^2x/\mathrm{d}t^2 + 2\cdot n{\cdot}\mathrm{d}x/\mathrm{d}t + p^2x = 0 \qquad (1)$$

where $n = C/(2{\cdot}m)$; $p^2 = k/m$
$k = k_0$ for $x \geq 0$
$k = \alpha \cdot k_0$ for $x < 0$ and $0 < \alpha \leq 1$

The values for C and k_0 were chosen to obtain the same natural frequency for the first mode,

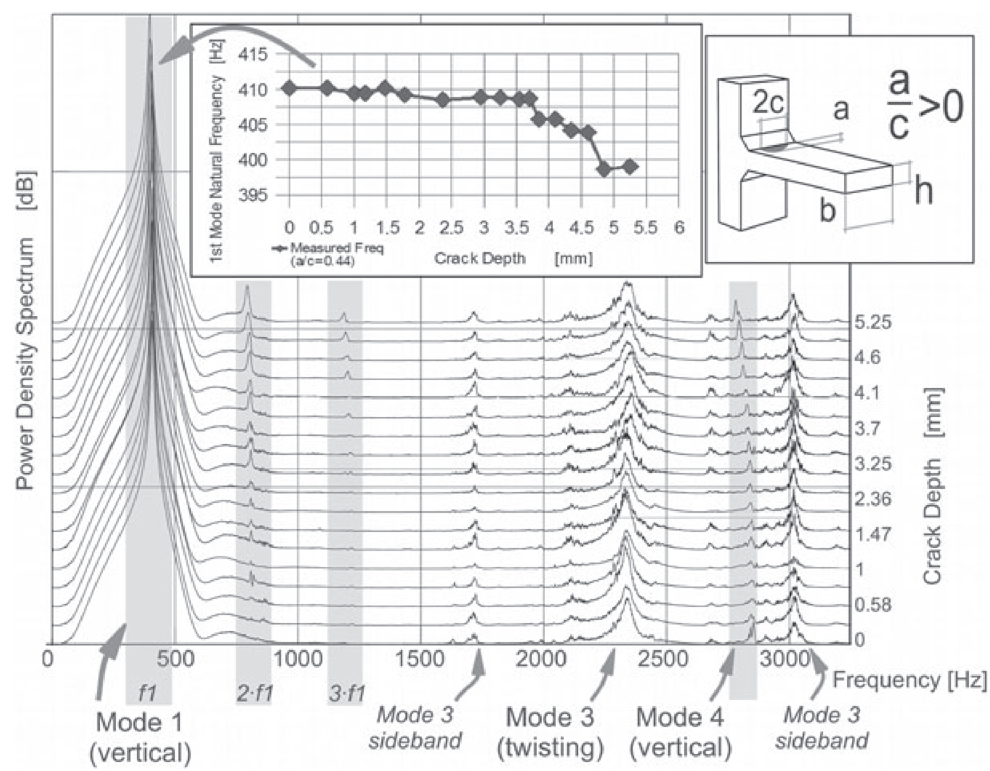

Figure 8 Stacked graph showing Averaged Power Spectrum Density for different stages of crack growth. The peaks for the first vertical vibrating modes and their sidebands are shown. The harmonics of the first natural frequency can be observed. The first natural frequency shift due to crack growth is shown on the top inset. The specimen geometry and crack shape is shown at the top right inset.

$p = 409$ Hz and damping $C = 20\ \mathrm{kg \cdot s^{-1}}$ as observed experimentally.

The equation above was solved for a 2-s length time vector using as initial conditions an imposed acceleration, $\mathrm{d}^2x/\mathrm{d}t^2(t=0) = A_0$, and null position and velocity, for two values of the bilinear parameter α: $\alpha = 1$ (no damage) and $\alpha = 0.99$ (1% of bending stiffness decrease). The Fast Fourier Transform algorithm was applied to the acceleration versus time results. Both results are shown in Fig. 9 along with the bilinear bending stiffness function $k(x)$. It can be observed that integer harmonics of the natural frequency arose as peaks in the power spectrum density (PSD) graph for $\alpha = 0.99$. From this, it can be concluded that the peaks found at multiples of the first bending mode frequency in Fig. 8 could be assumed to be the same bilinear behaviour as shown in Fig. 9.

Since harmonics of the first mode appeared in the PSD graph starting at a crack depth of 1 mm and crack detection using only natural frequency decrease was effective from 3.75 mm onwards, the method of inspection for harmonics appears to be a more useful tool for earlier fatigue-crack detection. A comparison between the detection thresholds for these two methods used in this work is shown in Fig. 10. It can be seen in this figure that the crack speed of growth at the lower threshold is about half of the growth speed at the higher threshold. This fact could give a bigger amount of time to take corrective actions before the component catastrophic failure.

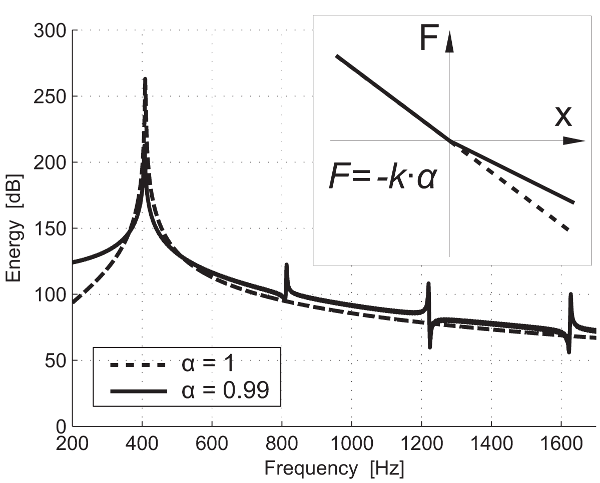

Figure 9 Power Spectral Density graph showing the theoretical impact response for a bilinear oscillator system with 1-d.f. The stiffness element function k varies through the parameter α as shown in the inset graph. Integer harmonics of the fundamental frequency arise when $\alpha < 1$.

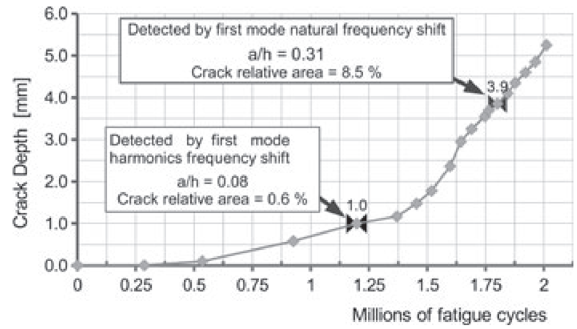

Figure 10 Graph showing crack depth versus number of fatigue cycles. The crack depth detection threshold for the detection of harmonics of the first natural frequency (threshold at 1 mm, 1.2 megacycles) was found lower than the measurement of the first natural frequency decrement (threshold at 3.85 mm, 1.8 megacycles).

Conclusions

In this work, the difference between fatigue cracks and through-thickness cuts on the free vibrating response of cantilever beams was studied using FEM and free vibration impact responses. The relation between fatigue cracks and sample width and the influence of the geometry of the through-thickness cuts on modelling results were studied. In addition, the spectral analysis technique was used and compared to natural frequencies shift inspection technique.

Test samples were made using two A36 steel plates welded in tee shape by the MIG process and cut in 47 mm width pieces.

A set of samples were through-thickness cut using a rotary saw to represent artificial cracks with aspect ratio $a/c = 0$. A different set of samples were submitted to alternating bending stress on the cantilever part to produce fatigue cracks by propagation under elastic regime. Impact response testing was done on both groups of samples every 0.5 mm of crack growth. Crack depth was measured on-line using an indirect strain gauge technique. Fast Fourier Transform algorithm was applied to the recorded data, from which natural frequencies corresponding to the normal modes of oscillation and PSD graphs were extracted.

Numerical modelling was done using the Finite Element Method using the sample geometry with both types of cracks. In addition, a numerical study of the influence of the width of the through-thickness cut was performed. An analysis of the influence of the sample width on the vibrating behaviour was done for geometries with fatigue cracks (aspect ratio $a/c = 0.45$).

Numerical modelling results were compared to experimental data for both types of damage.

Through-thickness cut geometries modelling results were closer to experimental data when the geometry used for modelling contained a cut whose dimensions were equal to those of the actual cut done on the test samples.

A breathing behaviour of the cracks was found on the fatigue-crack samples. This effect was confirmed using a numerical modelling using a 1-d.f. analytical solution for a bilinear stiffness spring element. The mentioned effect can be observed on PSD graphs as peaks at integer multiples of the natural frequency corresponding to the bending mode which affects the surface containing the crack mouth.

The vibration behaviour of the fatigue-cracked samples was found different to that of cut through-thickness samples when the crack mouth length is small in comparison to the sample width.

The detection threshold for cracks in samples was found to be earlier using frequency spectra than measuring natural frequencies shifts. A threshold of detection at less than $a/h = 0.1$ of relative crack depth (0.6% relative cross-sectional area loss) was achieved by inspecting integer harmonics, while the threshold of detection for natural frequency measurement was set at $a/h = 0.31$, representing 8.5% of cross-section loss. The most important aspect of the detection threshold found using harmonics is that the fatigue crack could be detected when its rate of growth is approximately 50% smaller than when measuring natural frequencies shifts.

Acknowledgments

The authors would like to thank Comisión Nacional de Investigación en Ciencia y Tecnología (CONICET) and Agencia Nacional de Promoción Científica y Tecnológica (ANPCyT) for supporting this work through grant PICT 06-534.

References

1. Cawley, P., and Adams, R.D., ''The Location of Defects in Structures from Measurements of Natural Frequencies,'' *Journal of Strain Analysis* **14**(2):49–55 (1979).
2. Dimarogonas, A., ''Vibration of Cracked Structures: A State of the Art Review,'' *Engineering Fracture Mechanics* **55**(5):831–857 (1996).
3. Nandwana, B.P., and Maiti, S.K., ''Detection of the Location and Size of a Crack in Stepped Cantilever Beams Based on Measurements of Natural Frequencies,'' *Journal of Sound and Vibration* **203**(3):435–446 (1997).
4. Kisa, M., and Brandon, J., ''The Effects of Closure of Cracks on the Dynamics of a Cracked Cantilever Beam,'' *Journal of Sound and Vibration* **238**(1):1–18 (2000).
5. Orhan, S., ''Analysis of Free and Forced Vibration of a Cracked Cantilever Beam,'' *NDT and E International* **40**:443–450 (2007).
6. Ruotolo, R., and Surace, C., ''Natural Frequencies of a Bar with Multiple Cracks,'' *Journal of Sound and Vibration* **272**:301–316 (2004).
7. Christides, S., and Barr, A.D.S. ''One-Dimensional Theory of Cracked Bernoulli-Euler Beams,'' *International Journal of Mechanics Science* **26**(11–12): 639–648 (1984).
8. Krawczuk, M., Palacz, M., and Ostachowicz, W., ''The Dynamic Analysis of a Cracked Timoshenko Beam by the Spectral Element Method,'' *Journal of Sound and Vibration* **264**:1139–1153 (2003).
9. Bamnios, Y., and Trochides, A., ''Dynamic Behaviour of a Cracked Cantilever Beam,'' *Applied Acoustics* **45**:97–112 (1995).
10. Dado, M., ''A Comprehensive Crack Identification Algorithm for Beams Under Different End Conditions,'' *Applied Acoustics* **51**(4):381–398 (1997).
11. Lin, H.-P., ''Direct and Inverse Methods on Free Vibration Analysis of Simply Supported Beams with a Crack,'' *Engineering Structures* **26**:427–436 (2004).
12. Bovsunovsky, A.P., and Matveev, V.V., ''Analytical Approach to the Determination of Dynamical Characteristics of a Beam with a Closing Crack,'' *Journal of Sound and Vibration* **235**(3):415–434 (2000).
13. Silva, J.M.M., and Gómez, A.J.M.A., ''Experimental Dynamic Analysis of Cracked Free-Free Beams,'' *Experimental Mechanics* **30**(1):20–25 (1990).
14. Bayly, P.V., ''On the Spectral Signature of Weakly Bilinear Oscillators,'' *Journal of Vibration and Acoustics* **118**:352–361 (1996).
15. Zhang, H., and Billings, S.A., ''Analysing Non-Linear Systems in the Frequency Domain-I: The Transfer Function,'' *Mechanic Systems and Signal Processing* **7**(6):531–550 (1993).
16. Owolabi, G.M., Swamidas, A.S.J., and Seshadri, R., ''Crack Detection in Beams Using Changes in Frequencies and Amplitudes of Frequency Response Functions,'' *Journal of Sound and Vibration* **265**:1–22 (2003).
17. Bamnios, Y., Douka, E., and Trochidis, A., ''Crack Identification in Beam Structures Using Mechanical Impedance,'' *Journal of Sound and Vibration* **256**(2):287–297 (2002).
18. Faverjon, B., and Sinou, J.-J., ''Robust Damage Assessment of Multiple Cracks Based on the Frequency Response Function and the Constitutive

Relation Error Updating Method,'' *Journal of Sound and Vibration* **312**:821–837 (2008).
19. Otegui, J.L., Mohaupt, U., and Burns, D., ''A Strain Gauge Technique for Monitoring Small Fatigue Cracks in Welds,'' *Engineering Fracture Mechanics* **40**(3):549–569 (1991).
20. Chapetti, M.D., *Propagación subcrítica de fisuras en aceros estructurales soldados*, Ph.D. Thesis, University of Mar del Plata, Argentina (1995).
21. Jaureguizahar, L.F., and Chapetti, M.D., ''Desarrollo de metodologías experimentales para la detección y monitoreo de propagación subcrítica de fisuras superficiales,'' *2nd Meeting of Young Researchers in Materials Science and Technology*, Materials Society of Argentina, 2008.
22. Eaton, J.W., Bateman, D., and Hauberg, S, Octave 3.0.1 Manual (2008).
23. Rosado, P., QtOctave 0.7.4 Reference Manual (2007).
24. Qian, S., and Chen, D., *Joint Time-Frequency Analysis: Methods and Applications.* Prentice-Hall Inc. (1996).